Electricity Tariff Aware Model Predictive Controller for Customer Battery Storage with Uncertain Daily Cycling Load

Dejan P. Jovanović, Gerard F. Ledwich, and Geoffrey R. Walker

***Abstract*—To optimally control the energy storage system of the battery exposed to the volatile daily cycling load and electricity tariffs, a novel modification of a conventional model predictive control is proposed. The uncertainty of daily cycling load prompts the need to design a new cost function which is able to quantify the associated uncertainty. By modelling a probabilistic dependence among flow, load, and electricity tariffs, the expected cost function is obtained and used in the constrained optimization. The proposed control strategy explicitly incorporates the cycling nature of customer load. Furthermore, for daily cycling load, a fixed-end time and a fixed-end output problem are addressed. It is demonstrated that the proposed control strategy is a convex optimization problem. While stochastic and robust model predictive controllers evaluate the cost concerning model constraints and parameter variations. Also, the expected cost across the flow variations is considered. The density function of load probability improves load prediction over a progressive prediction horizon, and a nonlinear battery model is utilized.**

***Index Terms*—Residential energy systems, battery storage, model predictive control, nonlinear optimization, cost of daily electricity consumption.**

I. Introduction

TO cover the cost of daily electricity consumption worldwide, it is necessary to allocate between 1% and 9% of the annual earnings [1]. Electricity tariffs significantly contribute to household electricity expenditures [2]. At the same time, electricity tariffs are necessary to cover the costs needed for the sustainable operation of the power grid [3]. However, some tariff scenarios may have a disruptive impact on a household budget depending on the load profile and socio-economic characteristics of the household [4]. The economic viability of different tariff schemes depends on the integration with a household battery energy storage system (BESS) [5]. In this paper, optimal BESS control strategy is examined which considers a probabilistic load profile, different tariff schemes and the cost-minimization for customers. One of the control strategies frequently used for BESS control is model predictive control (MPC), which is a cost-minimization iterative optimization method over a finite prediction horizon [6]. This strategy relies on the underlying process model. Regardless of its widespread use for BESS control, a conventional MPC (CMPC) does not directly include load profiles, different tariff schemes and optimized benefits of the customers. We present a novel modification of a CMPC which accommodates load variability, different tariff profiles and finally provide the globally optimal solution for the customer.

In [7], distributed and decentralized MPC of a residential BESS is designed. Load variability is flattened using averaging over the receding horizon. Terminal constraints are not considered. Reference [8] considers a rule-based MPC controller. Rules are based on the operation constraints of the BESS. The BESS control is defined as an optimal tracking problem, while the references are assumed to have smooth trajectories. In [9], an MPC-based approach is proposed to optimize the energy cost to the end-user. The two-stage strategy is developed separating the BESS control action between the energy deficit and excess. Load volatility is suppressed by introducing weights assigned to the cost of output error. In this way, customer benefits are significantly reduced. The inequality constraints are not imposed on a BESS. The concept of the end-user-driven microgrid is introduced in [10]. The end-user can consume and share the power only with the utility grid. A dynamic MPC-based optimization approach is used for optimal scheduling of power and battery energy. The method proposed in [11] combines an MPC with a Gaussian processes-based prediction for photovoltaic (PV) generation and demand. It is concluded that when the prediction is associated with the MPC, a shorter MPC horizon provides more accurate control. The prediction method outperforms the rule-based MPC algorithm. In [12], the MPC is applied to prevent the energy storage saturation. A mixed-integer multi-time scale stochastic optimization based on the MPC is proposed in [13] for a home energy management. The cost function is minimized subject to budget and power constraints, so that the indoor temperature is maintained at the reference level. In [14], a variable prediction horizon of MPC is applied to hybrid power systems. A

Manuscript received: May 13, 2020; revised: July 28, 2020; accepted: September 3, 2020. Date of CrossCheck: September 3, 2020. Date of online publication: June 25, 2021.

This work was supported by Australian Research Council (ARC) Discovery Project (No. 160102571).

D. P. Jovanović (corresponding author) is with the Institute of Electrical and Electronic Engineers, Queensland, Australia (e-mail: jovanovd@ieee.org).

G. F. Ledwich and G. R. Walker are with the School of Electrical Engineering and Robotics, Queensland University of Technology, Brisbane, Australia (e-mail: g.ledwich@qut.edu.au; geoffrey.walker@qut.edu.au).

DOI: 10.35833/MPCE.2020.000305

switched multiple-input multiple-output state-space model is proposed. To sum up, the load cycling variation is not considered in the existing literature. Also, load variability is neither explicitly modelled nor included in the control strategy. The receding horizon is assumed to have a fixed length, normally a day ahead. Finally, the convexity of the optimization strategy of the BESS is not explicitly demonstrated.

Model predictive controllers rely on dynamic models of the process [6]. Consequently, a BESS model has to facilitate the understanding of charging-discharging dynamics [15] and efficiencies [16], [17]. The modelling of the dynamics for different battery types is presented in [15]. The modelling of battery efficiency is complex and the results presented in [16] and [17] show that the internal energy losses when the energy is released in discharging are lower than the losses when the energy is consumed in charging [18]. The reduction of battery life is related to a very slow cumulative chemical process. Thus, the long-term effect can not be included in the strategy for battery control. Instead, the impact of battery utilization on its lifetime is accounted for by penalizing the battery charging value. The approximation is that the battery life is related to the energy processed, i.e., the total accumulated inflow of current over time [19]. The optimal battery sizing is considered in [20].

In the literature of end-user MPC-based battery control, a quadratic cost function is commonly accepted. The model generally used in the battery control is a state-space model. The cost function minimizes a distance between the model predictive output and a given set-point signal [6], [21]. The electricity price is not necessarily included in the quadratic cost function [8], [10], [14]. Alternatively, the electricity price is included without the assumption that the electricity price depends on energy flow [7], [11]-[13]. From the customer's viewpoint, the existing strategies do not directly address benefits for customers.

In this paper, we propose a novel globally optimal control strategy for household BESS affected by uncertain daily cycling load and electricity tariffs. Global optimality is achieved by using a new cost function that models a probabilistic dependence between flow, load and electricity tariffs. We prove that the expected value of the proposed cost function depends on the expected value of the net load and applied electricity tariffs. The electricity tariffs are modelled as a function of flow. Based on the newly proposed cost function, a novel modification of a CMPC is recommended. A horizon is of variable length since the battery usage is predominately defined by the peak load in the morning and evening. Finally, a model of a household BESS is a linear time-varying switching model since it depends on the energy flow direction. We propose a strategy that directly incorporates a switching model in the cost function. The block diagram of problem description is shown in Fig. 1.

The remainder of the paper is organized as follows. In Section II, the BESS modelling is described. Section III describes the methodology of the proposed BESS control. Results are given in Section IV and conclusions are presented in Section V.

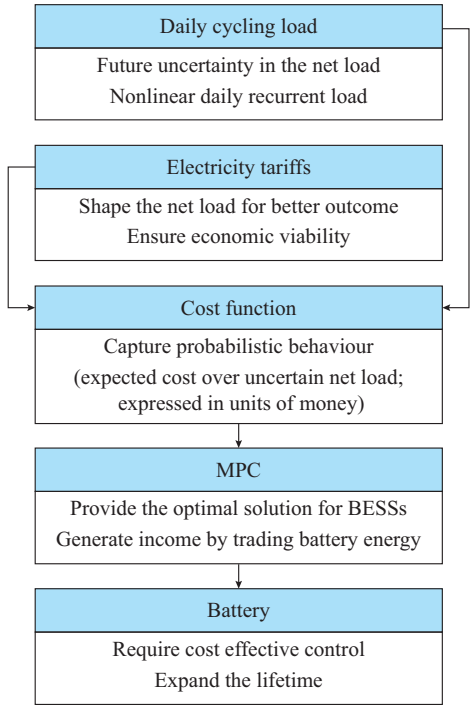

Fig. 1. Block diagram of problem description.

II. BESS Modelling

Subsystems that make up a BESS form a control unit, a communication link and a smart meter. A control unit regulates the energy stored in the batteries driven by a variable local demand and tariff rates. The existence of a communication link is assumed, across which the information about tariff changes is provided to the control unit in real time. A smart meter measures how much the energy is flowing between the power grid and a household equipped with a BESS. A simplified block diagram of the system is presented in Fig. 2, where $F(t)$ is the power exchanged with the power grid and measured by the smart meter; $L(t)$ is the net load defined as a difference between local demand and local generation; and $u(t)$ is the battery power controlled by the BESS. The main characteristics of the system are summarized in the following. The energy capacity of the BESS is given by E_c. Realistic modelling of the charging and discharging process of the battery requires realistic values for charging losses α^- and discharging losses α^+. The charging process is assumed less efficient than a discharging process [16], [17]. The maximum power rating of the converter is P_c.

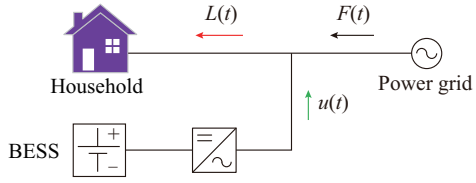

Fig. 2. A household with a BESS.

Based on these characteristics, a state-space model of the household BESS is given as:

$$E_{t+1} = E_t - \bar{\alpha} u_t \Delta T \tag{1}$$

where E_{t+1} is the instantaneous battery energy at time instance $t+1$; ΔT is a time interval during which a control signal u_t defines the instantaneous power delivered by a converter; and $\bar{\alpha}$ is defined as:

$$\bar{\alpha}=\begin{cases}\alpha^{+} & u_t>0\\ \alpha^{-} & u_t\le 0\end{cases} \tag{2}$$

In this paper, the losses in a battery are defined as a function of inverter efficiency since it is possible to map all the losses at the DC side of an inverter [8]. The state of charge of a battery system SOC_{t+1} [22], [23] is modelled by:

$$SOC_{t+1}=SOC_t-\frac{\bar{\alpha}u_t\Delta T}{E_c} \tag{3}$$

The application of complex battery models [15], [17] is not considered in this paper since it will not affect the overall design process.

Constraints are imposed on u_t, which requires that:

$$-P_c\le u_t\le P_c \tag{4}$$

Additionally, the minimum and maximum energy levels of the battery impose the constraints on acceptable values of instantaneous energy, so that the following relations can be obtained as:

$$E_{res}\le E_{t+1}\le E_c \tag{5}$$

where E_{res} is the contracted level of energy reserve required for bidding the BESS [24]. Finally, the constraint ensures that the energy level of BESS at the end of time horizon has the predefined value E_{end}:

$$E_{t_H}=E_{end} \tag{6}$$

where E_{t_H} is a fixed end output.

From (1) and (2), it follows that the underlying model of the system in Fig. 2 is a linear time-varying switching model since (1) depends on the power direction. Subsequently, the control of battery energy storage is a nonlinear control problem. Besides the nonlinearity, a control problem of battery energy storage is constrained with a set of operation limitations given by (4)-(6).

The power flow balance of the system in Fig. 2 is disrupted by cyclic random dynamics of the household net load. It is essential to incorporate those dynamics in the control method and evaluate the cost across the net load variability.

III. Progressive MPC (PMPC) for Uncertain Daily Cycling Load

In this section, the definition and properties of a novel modification of MPC are introduced. The problem is set as a nonlinear convex optimization problem constrained with the set of inequalities and equalities.

A. Properties of Proposed Optimal Strategy

As a convex optimization problem, MPC of the finite horizon $[t_1, t_H]$ is defined as:

$$\begin{cases}\min\limits_{\boldsymbol{u}} C(\boldsymbol{u})\\ \text{s.t. } \varphi_i(\boldsymbol{u})\le 0 \quad i=1,2,...,l\\ \quad\ \psi_j(\boldsymbol{u})=0 \quad j=1,2,...,m\end{cases} \tag{7}$$

where $C(\boldsymbol{u})$ is the cost function; $\boldsymbol{u}\in\mathbb{R}^H$ is the optimization (control) variable; $\varphi_i(\boldsymbol{u})$ is the convex function; and $\psi_j(\boldsymbol{u})$ is the affine function [25]. Since (1) is the forward difference approximation of the first derivative, it follows that the nonlinear constraints (5) are convex [25]. The equality constraint (6) is affine for the finite horizon $[t_1, t_H]$, since (1) can be rewritten as an affine transformation of the following form:

$$\boldsymbol{\Phi}(\boldsymbol{u})=\boldsymbol{A}\boldsymbol{u}+\boldsymbol{b} \tag{8}$$

where $\boldsymbol{A}=-\text{diag}\{\Delta T,...,\Delta T\}_{H\times H}$ is a linear transformation; $\boldsymbol{u}=[\bar{\alpha}u_1,\bar{\alpha}u_2,...,\bar{\alpha}u_H]^{\mathrm{T}}$ is the optimization (control) vector; and $\boldsymbol{b}=[E_{t_1},E_{t_2},...,E_{t_H}]^{\mathrm{T}}$. Note that at the finite horizon $[t_1, t_H]$, a fixed-end output E_{t_H} at a fixed-end time t_H can be written as:

$$E_{t_H}=E_{t_1}-\sum_{\tau=t_1}^{t_{H-1}}\bar{\alpha}u_\tau\Delta T \tag{9}$$

where u_τ is the component of $\boldsymbol{u}$ at the horizon point τ. With the constraints satisfying the convex optimization conditions, it remains to prove that the cost function is convex as well.

Generally, the total costs are determined by electricity tariffs and customer load. The total costs on the time interval $t\in[t_1, t_H]$ is defined as:

$$C_{tot}=\int_{t_1}^{t_H} g(F(t))\mathrm{d}t \tag{10}$$

where $g(F(t))$ is the integrand that represents an instantaneous cost, which depends on power flow and electricity tariffs:

$$g(F(t))=T(F(t))F(t) \tag{11}$$

where $T(F(t))$ is the function of flow $F(t)$, which models the electricity tariff. Since the main goal is to obtain a global optimal solution, the conditions of a convex optimization need to be verified. The first step is to prove that (11) is convex.

Theorem 1: an instantaneous cost (11) is a convex function.

Proof: for any sequence of flow $F(t)$ at time instances $t\in\{t_1,t_2,...,t_n\}$ and set of positive constants $0<\eta_i<1$, $i\in\{1,2,...,n\}$, function (11) can be written as:

$$g\left(\sum_{i=1}^{n}\eta_i F(t_i)\right)=T\left(\sum_{i=1}^{n}\eta_i F(t_i)\right)\sum_{i=1}^{n}\eta_i F(t_i) \tag{12}$$

Assuming that for each individual flow instance, $F(t_i)$ is possible to choose its own tariff rate $T(F(t_i))>0$, so that the following can be obtained as:

$$g\left(\sum_{i=1}^{n}\eta_i F(t_i)\right)=T\left(\sum_{i=1}^{n}\eta_i F(t_i)\right)\sum_{i=1}^{n}\eta_i F(t_i)\le \sum_{i=1}^{n}\eta_i T(F(t_i))F(t_i)=\sum_{i=1}^{n}\eta_i g(F(t_i)) \tag{13}$$

Since the inequality (13) has the form of Jensen's inequality [25], then the convexity of (11) follows.

By a theorem of calculus [26], which states that an integral of a convex function is also convex, and theorem 1, it follows that the integral (10) is a convex function. Therefore, it follows that the proposed strategy defined by (7)-(10) is a convex optimization problem which guarantees that every local minimum is a global minimum [25].

B. Expected Cost Function

Generally, $T(F(t))$ could assume multiple electricity tariff rates. However, to simplify the theoretical considerations, a particular case of two electricity tariff rates is evaluated as:

$$T(F(t))=\begin{cases}T_0 & F(t)<0\\ T_1 & F(t)\geq 0\end{cases} \tag{14}$$

where T_0 is the feed-in tariff; and T_1 is the grid-spot tariff. The difficulty with a direct calculation of the total costs in (10) is related to the random behaviour of the load. Consequently, to optimize an integral (10), an operator of mathematical expectation needs to be applied to it. As a result, the following equation is obtained:

$$\mathbb{J}=\mathbb{E}\{C_{tot}\}=\mathbb{E}\left\{\int_{t_1}^{t_H} g(F(t))\mathrm{d}t\right\} \tag{15}$$

where $\mathbb{J}$ is the performance index calculated as the expected value of the total cost; and $\mathbb{E}$ is the operator of the mathematical expectation. Interchanging the integral with the expectation is possible if and only if an integrand $g(F)$ is bounded [27]. The condition is satisfied since all variables in $g(F)$ are constrained by their maximum values. After interchanging the integral with the expectation and by approximating the integral with a sum, (15) becomes:

$$\mathbb{J}=\mathbb{E}\{C_{tot}\}=\sum_{\tau=1}^{H}\mathbb{E}\{g_\tau(F)\}\Delta T \tag{16}$$

where $g_\tau(F)$ is defined as in (11) but computed at time τ. It follows that the problem of calculation of $\mathbb{J}$ comes down to calculate the mathematical expectation of $g_\tau(F)$. The expected value of a function is given as:

$$\mathbb{E}\{g_\tau(F)\}=\int_F g_\tau(F)p_F\mathrm{d}f \tag{17}$$

where p_F is the probability density function (PDF) of a random variable F. The expectation in its unfolded form is based on (4), which is given as:

$$\mathbb{E}\{g_\tau(F)\}=T_0\int_{-\infty}^{0} fp_F\mathrm{d}f+T_1\int_0^{\infty} fp_F\mathrm{d}f \tag{18}$$

The expectation of the instantaneous cost is split into two integrals. The integrals quantify the cost of expected values of a negative and a positive power flow component. The compact form of (18) is given as:

$$\mathbb{E}\{g_\tau(F)\}=T_0\mathbb{E}\{F_-\}\mathbb{I}_{\{F<0\}}+T_1\mathbb{E}\{F_+\}\mathbb{I}_{\{F\geq 0\}} \tag{19}$$

where $\mathbb{I}_{\{\cdot\}}$ is the indicator function for given condition. The expectations $\mathbb{E}\{F_-\}$ and $\mathbb{E}\{F_+\}$ depend on grid flow F. In addition, based on Fig. 2, the power flow $F(t)$ is a function of load $L(t)$ and battery flow $u(t)$. The flow balance equation $F_{k|t}$ from Fig. 2 is given as:

$$F_{k|t}=L_{k|t}-u_{k|t} \tag{20}$$

where t is the real-time instance at which the system variables are measured; k is the simulation index denoting the MPC prediction step with respect to t; $L_{k|t}$ is the net load; and $u_{k|t}$ is the battery flow. Since $u_{k|t}$ is a result of the MPC algorithm from previous control period $t-1$, the value of $u_{k|t}$ is known and fixed at a time when the integral (18) is calculated, so that the value of $u_{k|t}$ is fixed for the purpose of evaluation in (20). A change of variables in (18) using (20) transforms the expectations $\mathbb{E}\{F_-\}$ and $\mathbb{E}\{F_+\}$ into:

$$\mathbb{E}\{F_-\}=\int_{-\infty}^{0} f_{k|t}p_F(f_{k|t})\mathrm{d}f_{k|t}=\int_{-\infty}^{u_{k|t}}(l_{k|t}-u_{k|t})p_F(l_{k|t}-u_{k|t})\mathrm{d}f_{k|t} \tag{21}$$

$$\mathbb{E}\{F_+\}=\int_{0}^{\infty} f_{k|t}p_F(f_{k|t})\mathrm{d}f_{k|t}=\int_{u_{k|t}}^{\infty}(l_{k|t}-u_{k|t})p_F(l_{k|t}-u_{k|t})\mathrm{d}f_{k|t} \tag{22}$$

Given the relation (20) between random variables F and L, it is required to define a relation between the cumulative distribution functions (CDFs) Φ_L and Φ_F. The CDF of a real-valued random variable X is defined as $\Phi_X(x)=P(X\leq x)$ [28]. The relation between CDFs is obtained as:

$$\Phi_L(l)=P(L\leq l)=P(F+u\leq l)=P(F\leq l-u)=\Phi_F(l-u) \tag{23}$$

From (23), it follows that the relation between PDFs for F and L is given by $p_L(l)\mathrm{d}l=p_F(l-u)\mathrm{d}f$. Also, assuming that $u_{k|t}$ is constant and independent from $l_{k|t}$, it follows from (23) that $\mathrm{d}l=\mathrm{d}f$. Finally, the expressions for expected values in (24) and (26) transform to the following equation:

$$\begin{aligned}\mathbb{E}\{F_-\}&=\int_{-\infty}^{u_{k|t}}(l_{k|t}-u_{k|t})p_L(l_{k|t})\mathrm{d}l_{k|t}=\int_{-\infty}^{u_{k|t}} l_{k|t}p_L(l_{k|t})\mathrm{d}l_{k|t}-\\ &\quad u_{k|t}\int_{-\infty}^{u_{k|t}} p_L(l_{k|t})\mathrm{d}l_{k|t}=\mathbb{E}_{u_{k|t}}\{L_-\}-\alpha_{u_{k|t}}u_{k|t}\end{aligned} \tag{24}$$

$$\begin{aligned}\mathbb{E}\{F_+\}&=\int_{u_{k|t}}^{\infty}(l_{k|t}-u_{k|t})p_L(l_{k|t})\mathrm{d}l_{k|t}=\int_{u_{k|t}}^{\infty} l_{k|t}p_L(l_{k|t})\mathrm{d}l_{k|t}-\\ &\quad u_{k|t}\int_{u_{k|t}}^{\infty} p_L(l_{k|t})\mathrm{d}l_{k|t}=\int_{u_{k|t}}^{\infty} l_{k|t}p_L(l_{k|t})\mathrm{d}l_{k|t}-\\ &\quad u_{k|t}\left(1-\int_{-\infty}^{u_{k|t}} p_L(l_{k|t})\mathrm{d}l_{k|t}\right)=\mathbb{E}_{u_{k|t}}\{L_+\}-(1-\alpha_{u_{k|t}})u_{k|t}\end{aligned} \tag{25}$$

where $\mathbb{E}_{u_{k|t}}\{L_-\}$, $\mathbb{E}_{u_{k|t}}\{L_+\}$ and $\alpha_{u_{k|t}}$ are calculated as:

$$\mathbb{E}_{u_{k|t}}\{L_-\}=\int_{-\infty}^{u_{k|t}} l_{k|t}p_L(l_{k|t})\mathrm{d}l_{k|t} \tag{26}$$

$$\mathbb{E}_{u_{k|t}}\{L_+\}=\int_{u_{k|t}}^{\infty} l_{k|t}p_L(l_{k|t})\mathrm{d}l_{k|t} \tag{27}$$

$$\alpha_{u_{k|t}}=\int_{-\infty}^{u_{k|t}} p_L(l_{k|t})\mathrm{d}l_{k|t} \tag{28}$$

To compute the expected values (26) and (27) and the weighting factor (28), given an arbitrary load PDF $p_L(l_{k|t})$, Markov chain Monte Carlo (MCMC) methods can be used. However, in the following for the sake of computation simplicity, a random load is modelled with Gaussian distribution $L_{k|t}\sim\mathcal{N}(\mu_{k|t},\sigma_{k|t}^2)$, where $\mu_{k|t}$ and $\sigma_{k|t}$ are the parameters of Gaussian distributions.

C. Comparative Study of Simulation-based Cost Function

The calculation of (19) is required in the the expected cost function (16) at every real-time instance. Based on the calculation, the optimal control action sequence of MPC is obtained. To demonstrate the advantages of the newly proposed cost function, it needs to be compared with a cost function used in a CMPC which is based on (20). Therefore, the net load $L_{k|t}$ is substituted with the average value of net load $\mu_{L_{k|t}}$. This type of cost function is called the expected load cost function.

To quantify the differences between cost functions, a synthesized example is created when a sudden jump in demand happens, so that the demand is higher than the generation. In the case of expected cost function, the probabilistic net load is modelled with the Gaussian distribution with $\mu_L = 1$ kW and the parameter $\sigma_L \in \{0.5, 1, 1.5\}$. In the case of the expected load cost function, only the mean value $E\{L_{k|t}\} = \mu_L$ is used as the predicted net load value. In both cases, the prediction horizon is 24 hours. For the Gaussian distribution, integrals (26) and (27) can be calculated algebraically applying the following equation:

$$\mathbb{E}\{X\} = \frac{1}{\sigma\sqrt{2\pi}} \int_{\alpha}^{\beta} x \mathrm{e}^{-\frac{(x-\mu)^2}{2\sigma^2}} \mathrm{d}x \Bigg|_{z=\frac{x-\mu}{\sigma}} = \frac{1}{\sigma\sqrt{2\pi}} \int_{p}^{q} (\sigma z + \mu) \mathrm{e}^{\frac{z^2}{2}} \sigma z \mathrm{d}z = \sigma \sqrt{\frac{2}{\pi}} (\mathrm{e}^{-0.5p^2} - \mathrm{e}^{-0.5q^2}) + \frac{\mu}{2} \left(erf\left(\frac{q}{\sqrt{2}}\right) - erf\left(\frac{p}{\sqrt{2}}\right) \right) \tag{29}$$

where μ and σ are the parameters of Gaussian distribution used to calculate the expected value of the random variable X; $p = (\alpha - \mu)/\sigma$; and $q = (\beta - \mu)/\sigma$. Similarly, the integral in (28) can be calculated by:

$$\alpha_{u_{k|t}} = \frac{1}{2} \left[erf\left(\frac{r}{\sqrt{2}}\right) + 1 \right] \tag{30}$$

where $r = (u_{k|t} - \mu_L)/\sigma_L$. It is worth noting that the expected cost depends on two parameters μ_L and σ_L, while the expected load cost function solely depends on μ_L.

In Fig. 3, battery control values are presented to illustrate the essential difference between the two types of cost functions. The response to the sudden increase in demand is obtained by using the expected load cost function, which shows that the battery is discharged only to match the demand. For the expected load cost function, the battery charging happens before and after demand increases. The battery response obtained by applying the expected cost function exhibits different behaviours, i. e., the battery is discharged above the demand for considered cases and the level of the discharging depends on the Gaussian distribution parameter σ_L. For smaller values of σ_L, higher discharging is achieved. In Fig. 4, battery energy values are presented, demonstrating that the expected cost function enables higher charging energy compared with the expected load cost function.

Figure 5 illustrates the calculation of expected cost flow. For the expected load cost function which depends only on μ_L, the expected cost flow is the linear function of battery control. For the expected cost strategy, the expected cost flow is a nonlinear function of battery control. As the battery control approaches μ_L, the expected positive flow is proportionally increasing with σ_L. Contrarily, the expected negative flow is decreasing as σ_L increases.

In conclusion, waveforms of battery control signals in Fig. 3 are the results of the optimization process, minimizing the power exchanged with the power grid. The expected cost approach is demonstrated with more flexibility. Based on the expected cost function in the following subsection, the variable length horizon of MPC methodology is proposed to deal with the explicit cycling nature of the load.

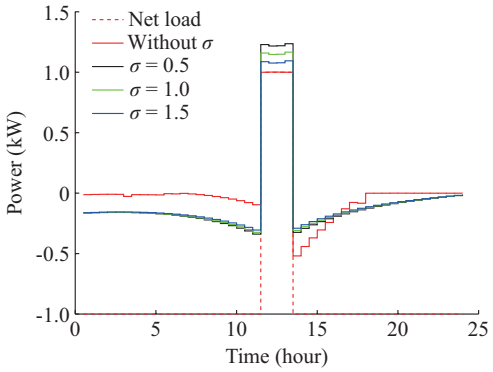

Fig. 3. Battery control values for expected cost and expected load cost functions.

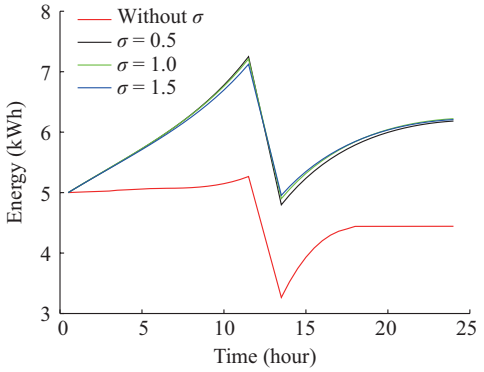

Fig. 4. Battery energy values for expected cost and expected load cost functions.

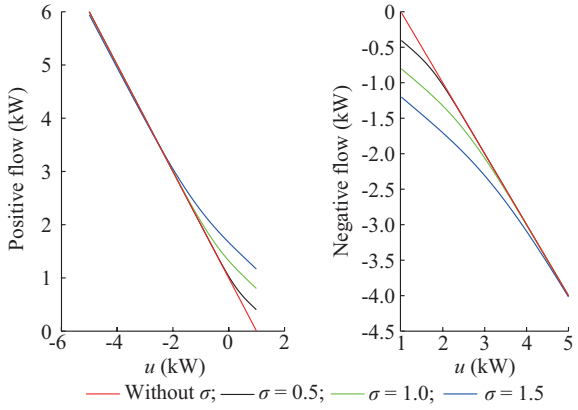

Fig. 5. Calculation of expected cost flow.

D. PMPC

In conventional MPC [6], the end of the horizon is shifted towards the future at each time instance. The resulting control sequence is bounded by a set of constraints, both inequality and equality. One of the limitations of applying the equality constraints to a CMPC for daily cycling load control is that the value at the end of horizon affects the control sequence. Since the horizon is passing through intervals with different values of load imbalance, it follows that the control

sequence will depend on load value at the end of the horizon. However, in the case of the household with a BESS with the cycling nature of the load, a different strategy is required. Compared with the CMPC, the proposed control strategy assumes that the end of the horizon is fixed and finishes at a low power time. This assumption is justified by the fact that the load profile, on average, has a 24-hour recurrent interval. Consequently, the battery usage is predominantly defined by the peaks in the morning and evening, while after the peak in the evening, the battery usage is less demanding. In this way, the horizon is reducing while progressing towards the end of a recurrent interval. This control strategy is called PMPC since the horizon duration is variable and finally stops at a low value of battery demand.

The algorithm steps are summarized in Algorithm 1. As the inputs, the algorithm takes the previously computed control sequence $[u_{k|t}]$, $k=1,2,\ldots,H$ and the predicted load $[\hat{\mu}_{L_{k|t}}, \hat{\sigma}_{L_{k|t}}]$, $k=1,2,\ldots,H$ on the finite horizon H.

Algorithm 1: PMPC

1. Procedure of PMPC: $[u_{k|t}]$, $[\hat{\mu}_{L_{k|t}}, \hat{\sigma}_{L_{k|t}}]$, $k=1,2,\ldots,H$
2. $\mathbb{E}\{g_{k|t}(F)\} = T_0\mathbb{E}\{F_-\}\mathbb{I}_{\{F<0\}} + T_1\mathbb{E}\{F_+\}\mathbb{I}_{\{F\geq 0\}}$
3. $\mathbb{E}\{C_{tot}\} = \sum_{k=1}^{H}\mathbb{E}\{g_{k|t}(F)\}\Delta T - \lambda u_{k|t}\mathbb{I}_{\{u_{k|t}<0\}}$
4. $\min_{u_{1|t+1},\ldots,u_{H|t+1}} \mathbb{E}\{C_{tot}\}$
5. **return** $u_{1|t+1}$
6. End procedure

As stated before, to increase the battery life, it is important to penalize the inflow variability. To achieve this goal, the expected cost function (16) is extended by adding a penalty term $-\lambda u_{k|t}\mathbb{I}_{\{u_{k|t}<0\}}$ for inflows, where λ is a weighting factor and the negative sign makes the penalty term positive, as shown in lines 3 and 4 of Algorithm 1. As a result, the control sequence $[u_{k|t}]$, $k=1,2,...,H$ is calculated. As with the CMPC [6], from the sequence obtained, only the first control signal $u_{1|t+1}$ is used by the battery controller.

Note that the computation time of the proposed control strategy is determined by three major contributors as stated in [29]. The results in the following section are obtained using the interior point optimization method which takes the advantage of the convex cost function.

IV. Results

The advantages of the PMPC over the CMPC are demonstrated in this section. The PMPC is based on the expected cost function and the fixed-end horizon, while the CMPC applies the expected load cost function and a fixed 24-hour prediction horizon. Both of them are tested using the same BESS model (1), whose parameters are summarized in Table I. The loss terms in (2) are calculated based on the loss coefficient α, which are $\alpha^- = \alpha = 0.96$ [30] and $\alpha^+ = \alpha^{-1} = 1.0417$.

The PV generation is modelled by average daily curve [31]. Considering the load demand, the generic profile type 2 [32] is used with well-defined peak loads in the morning and evening.

TABLE I
Parameters of BESS Model

P_c (kW)	E_c (kWh)	E_{res} (kWh)	E_{end} (kWh)	α	ΔT (hour)
5	10	2	5	0.96	0.5

The net load is defined as a difference between a household demand and PV generation, as shown in Fig. 6. The flat electricity tariffs are applied. The feed-in tariff T_0 is 0.05 \$/kWh while the grid-spot tariff T_1 is 0.25 \$/kWh.

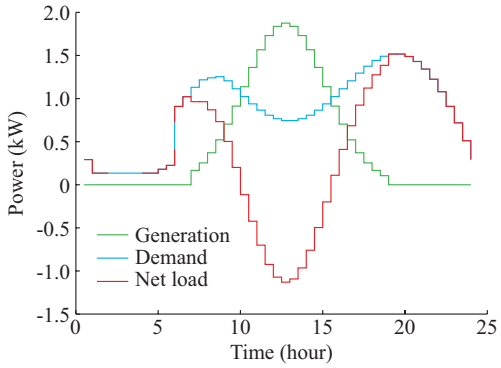

Fig. 6. Daily PV generation, a household demand and net load.

The CMPC and PMPC are compared for the net load given in Fig. 6. The control actions are presented in Fig. 7. In Fig. 7, u_{CMPC} and u_{PMPC} are the control actions for CMPC and PMPC, respectively. The control sequence obtained by the CMPC based on the expected load cost function consistently attempts to follow the net load. In the case when it is not feasible, the control action reduces to smaller values. The most significant issue is that the CMPC is missing out to support the power grid during the peak time in the morning and evening. The PMPC supports the power grid during the peak time. Besides, the advantage of the PMPC over the CMPC is the ability of PMPC to additionally charge the BESS during a day when additional energy is available due to PV generation.

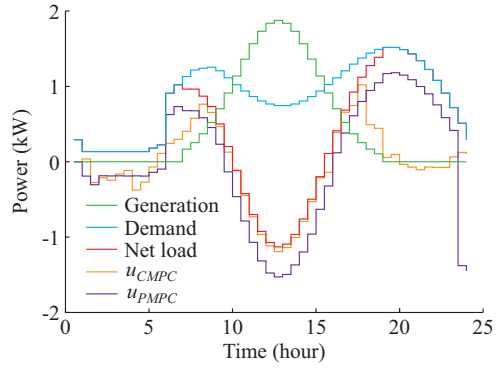

Fig. 7. Control actions for CMPC and PMPC.

As a result of applying different cost functions, the obtained control sequences result in different dynamical behaviour for a household BESS. Battery energy level presented in Fig. 8 shows that the control strategy of PMPC has two main advantages over the CMPC. E_{CMPC} and E_{PMPC} are the

energy storages for CMPC and PMPC, respectively. Firstly, the amount of the energy which is stored in the battery during a day reaches the maximum level allowed by the imposed constraint ($E_c \leq 10$ kWh). Secondly, the energy levels at the end of a day are different. Whilst the battery energy level for PMPC satisfies the fixed-end point constraint ($E_{end} = 5$ kWh), it is impossible to control the energy level achieved by the CMPC at the same time instance. The fixed 24-hour prediction horizon does not allow the fixed-end point control in the case of a daily cycling load.

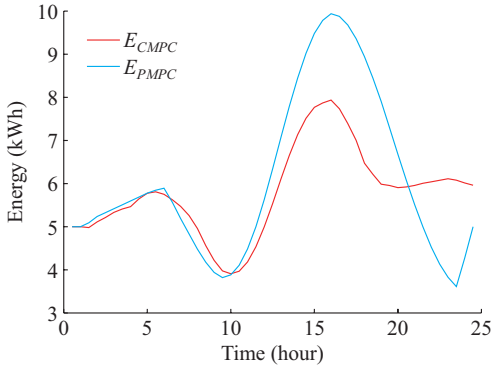

Fig. 8. Battery energy level for CMPC and PMPC.

The insights into predicted control sequences for both CMPC and PMPC are presented in Figs. 9 and 10, respectively, which show the control sequence $u_{k|t}$ for different t and k. For the CMPC, each control sequence has the 24-hour prediction horizon, while the prediction horizon of PMPC ends at a fixed-end point, which is the midnight for this case.

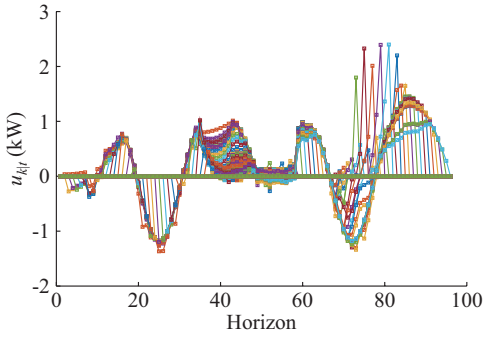

Fig. 9. Predicted control sequence of CMPC.

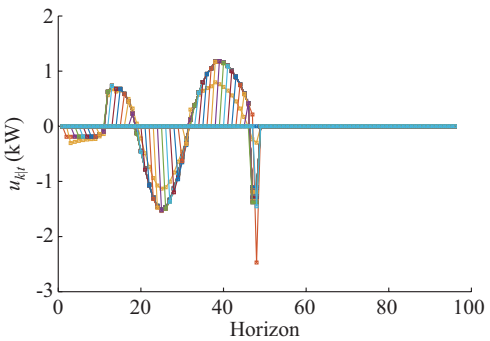

Fig. 10. Predicted control sequence of PMPC.

In Fig. 9, two types of responses in the predicted control sequence are observed. Initially, the control sequence is reasonably smooth (the horizon indexes between 1 and 34). However, the predicted control signal exhibits abrupt changes. The main reason is that the predicted net load starts to have both the intervals with positive and negative values. Therefore, the CMPC makes a decision to average the predicted control sequence in response to the changes of signs in the net load. As the result, the CMPC decides to stop discharging the BESS and even to start charging the BESS during the peak time in the evening. In Fig. 10, the predicted control sequence of PMPC is smooth except for the last few samples when PMPC attempts to satisfy the fixed-end constraint $E_{end} = 5$ kWh. The main advantage of the PMPC with expected cost function over the CMPC with the expected load function is that it successfully controls the fixed-end constraint by incorporating the cycling nature of the load. The control actions of CMPC and PMPC for noisy generation and demand are presented in Figs. 11 and 12, respectively.

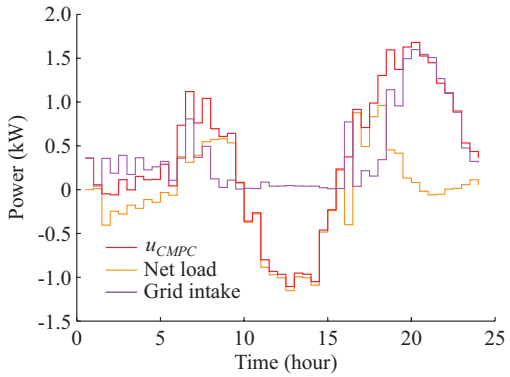

Fig. 11. Control action of CMPC for noisy generation and demand.

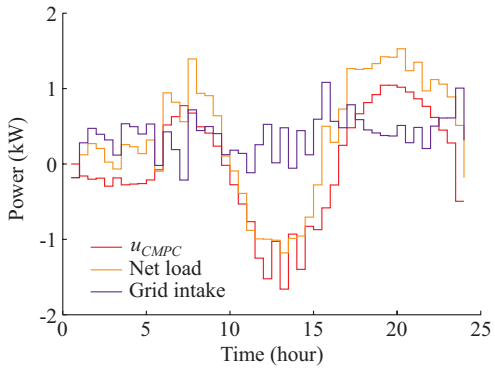

Fig. 12. Control action of PMPC for noisy generation and demand.

Note that the time-of-use (TOU) price and dynamic rates can be considered as well using the proposed control strategy by adapting (14). These rates are defined as the tariff pairs $T(F(t)) \in \{[T_0^1, T_1^1], [T_0^2, T_1^2], \ldots, [T_0^{N-1}, T_1^{N-1}]\}$. The strategy operates in the same way as for the flat tariffs and avoids energy purchase during the peak time.

The last group of the results demonstrates the advantages of the newly proposed control strategy in the presence of noise, which has the standard normal distribution with stan-

dard deviation as $\sigma = 0.125$. The assumption is that both daily PV generation and demand are affected by random interference. The random PV generation models the change of weather conditions, while the random demand models the variability of a household consumption. In order to assess the benefits of the PMPC, it is necessary to generate multiple random realizations for both the PV generation and demand. Using Monte Carlo experiments, a hundred realizations are generated and the evaluation of the CMPC and the PMPC are obtained. The battery energy level for CMPC and PMPC for noisy generation and demand is shown in Fig. 13.

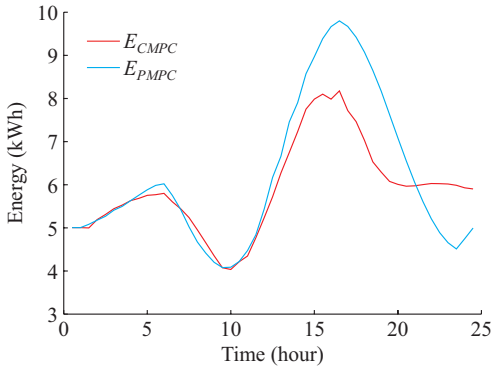

Fig. 13. Battery energy level for CMPC and PMPC for noisy generation and demand.

The benefits of PMPC with expected cost function is summarized in Fig. 14, where the histograms are plotted together with estimated PDFs. The mean and standard deviations corresponding to the CMPC μ_{CMPC} and σ_{CMPC} are \$5.11 and \$0.29, respectively. The blue line is the Gaussian PDF for μ_{CMPC}. Similar, the red line is Gaussian PDF for σ_{CMPC}.

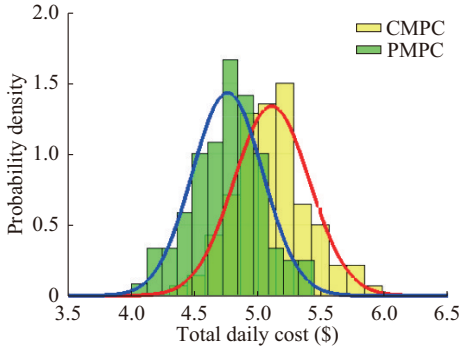

Fig. 14. Benefits of PMPC with expected cost function.

The mean and standard deviations for the PMPC μ_{PMPC} and σ_{PMPC} are \$4.76 and \$0.28, respectively, implying that the PMPC with the expected cost function has a smaller total cost compared with that of the CMPC with the expected load cost function.

V. Conclusion

To optimally control a household BESS, a novel modification of an MPC is proposed. A probabilistic evaluation of a new cost function incorporates the random nature of cycling customer load, intermittent nature of the PV generation and variable tariffs. The probabilistic calculation of the cost function is applied on the horizon whose length changes progressively. A progressive horizon technique includes a fixed-end time and a fixed-end output. It is shown that for such constraints defined, an optimization problem has a globally optimal solution. Economic viability of the proposed control strategy is demonstrated using Monte Carlo experiments.

Finally, the proposed control strategy enables a household daily cost reduction in the presence of electricity tariffs and an uncertain daily cycling load.

Future work will include load prediction analysis using different PDFs and their expected values. Additionally, the coordination of multiple household battery packs will be considered. Also, the application of unsupervised learning algorithms for the adaptation of load PDF will be investigated.

References

[1] OECD. (2019, Jan.). Purchasing power parities (PPP) (indicator). [Online]. Avalable: https://data. oecd. org/conversion/purchasing-power-parities-ppp.htm

[2] V. Venizelou, N. Philippou, M. Hadjipanayi *et al.*, "Development of a novel time-of-use tariff algorithm for residential prosumer price-based demand side management," *Energy*, vol. 142, pp. 633-646, Jan. 2018.

[3] E. Klaassen, C. Kobus, J. Frunt *et al.*, "Responsiveness of residential electricity demand to dynamic tariffs: experiences from a large field test in the netherlands," *Applied Energy*, vol. 183, pp. 1065-1074, Dec. 2016.

[4] V. Azarova, D. Engel, C. Ferner *et al.*, "Exploring the impact of network tariffs on household electricity expenditures using load profiles and socio-economic characteristics," *Nature Energy*, vol. 3, pp. 317-325, Apr. 2018.

[5] G. Brusco, A. Burgio, D. Menniti *et al.*, "The economic viability of a feed-in tariff scheme that solely rewards self-consumption to promote the use of integrated photovoltaic battery systems," *Applied Energy*, vol. 183, pp. 1075-1085, Dec. 2016.

[6] E. Camacho and C. Bordons, *Model Predictive control*. London: Springer, 2007.

[7] K. Worthmann, C. M. Kellett, P. Braun *et al.*, "Distributed and decentralized control of residential energy systems incorporating battery storage," *IEEE Transactions on Smart Grid*, vol. 6, no. 4, pp. 1914-1923, Jul. 2015.

[8] S. Teleke, M. E. Baran, S. Bhattacharya *et al.*, "Rule-based control of battery energy storage for dispatching intermittent renewable sources," *IEEE Transactions on Sustainable Energy*, vol. 1, no. 3, pp. 117-124, Oct. 2010.

[9] A. Mahamadi and S. Sastry, "Model predictive controller for battery management systems," in *Proceedings of 2015 International Conference on Computing, Control, Networking, Electronics and Embedded Systems Engineering (ICCNEEE)*, Khartoum, Sudan, Sept. 2015, pp. 21-26.

[10] T. G. Paul, S. J. Hossain, S. Ghosh *et al.*, "A quadratic programming based optimal power and battery dispatch for grid-connected microgrid," *IEEE Transactions on Industry Applications*, vol. 54, no. 2, pp. 1793-1805, Mar. 2018.

[11] J. Lee, P. Zhang, L. K. Gan *et al.*, "Optimal operation of an energy management system using model predictive control and gaussian process time-series modeling," *IEEE Journal of Emerging and Selected Topics in Power Electronics*, vol. 6, no. 4, pp. 1783-1795, Dec. 2018.

[12] E. Perez, H. Beltran, N. Aparicio *et al.*,"Predictive power control for PV plants with energy storage," *IEEE Transactions on Sustainable Energy*, vol. 4, no. 2, pp. 482-490, Apr. 2013.

[13] Z. Yu, L. Jia, M. C. Murphy-Hoye *et al.*, "Modeling and stochastic control for home energy management," *IEEE Transactions on Smart Grid*, vol. 4, no. 4, pp. 2244-2255, Dec. 2013.

[14] B. Zhu, H. Tazvinga, and X. Xia, "Switched model predictive control for energy dispatching of a photovoltaic-diesel-battery hybrid power system," *IEEE Transactions on Control Systems Technology*, vol. 23, no. 3, pp. 1229-1236, May 2015.

[15] O. Tremblay and L. A. Dessaint, "Experimental validation of a battery dynamic model for EV applications," *World Electric Vehicle Journal*, vol. 3, no. 2, pp. 289-298, Jun. 2009.

[16] J. B. Copetti, E. Lorenzo, and F. Chenlo, "A general battery model for PV system simulation," *Progress in Photovoltaics: Research and Applications*, vol. 1, no. 4, pp. 283-292, Apr. 1993.
[17] J. F. Manwell and J. G. McGowan, "Extension of the kinetic battery model for wind/hybrid power systems," in *Proceedings of European Wind Energy Conference and Exhibition (EWEC)*, Thessaloniki, Greece, pp. 284-289, Jun. 1994.
[18] K. Li and K. J. Tseng, "Energy efficiency of lithium-ion battery used as energy storage devices in micro-grid," in *Proceedings of IECON 2015–41st Annual Conference of the IEEE Industrial Electronics Society*, Yokohama, Japan, Nov. 2015, pp. 5235-5240.
[19] S. B. Peterson, J. Apt, and J. Whitacre, "Lithium-ion battery cell degradation resulting from realistic vehicle and vehicle-to-grid utilization," *Journal of Power Sources*, vol. 195, no. 8, pp. 2385-2392, Aug. 2010.
[20] X. Wu, X. Hu, X. Yin *et al*., "Optimal battery sizing of smart home via convex programming," *Energy*, vol. 140, pp. 444-453, Dec. 2017.
[21] L. Wang, *Model Predictive Control System Design and Implementation Using MATLAB*. London: Springer, 2009.
[22] C. Bian, H. He, S. Yang *et al*., "State-of-charge sequence estimation of lithium-ion battery based on bidirectional long short-term memory encoder-decoder architecture," *Journal of Power Sources*, vol. 449, p. 227558, Feb. 2020.
[23] X. Hu, H. Jiang, F. Feng *et al*., "An enhanced multi-state estimation hierarchy for advanced lithium-ion battery management," *Applied Energy*, vol. 257, p. 114019, Jan. 2020.
[24] M. Merten, C. Olk, I. Schoeneberger *et al*., "Bidding strategy for battery storage systems in the secondary control reserve market," *Applied Energy*, vol. 268, p. 114951, Jun. 2020.
[25] S. Boyd and L. Vandenberghe, *Convex Optimization*. Cambridge: Cambridge University Press, 2004.
[26] M. J. Cloud, B. C. Drachman, and L. P. Lebedev, *Inequalities With Applications to Engineering*. New York: Springer International Publishing, 2014.
[27] W. R. Wade, "The bounded convergence theorem," *The American Mathematical Monthly*, vol. 81, no. 4, pp. 387-389, Apr. 1974.
[28] G. Grimmett and D. Stirzaker, *Probability and Random Processes*. Oxford: Oxford University Press, 2008.
[29] S. Richter, C. N. Jones, and M. Morari, "Computational complexity certification for real-time MPC with input constraints based on the fast gradient method," *IEEE Transactions on Automatic Control*, vol. 57, no. 6, pp. 1391-1403, Nov. 2012.
[30] T. Kerekes, R. Teodorescu, P. Rodriquez *et al*., "A new high-efficiency single-phase transformerless PV inverter topology," *IEEE Transactions on Industrial Electronics*, vol. 58, no. 1, pp. 184-191, Jan. 2011.
[31] S. Pfenninger and I. Staffell, "Long-term patterns of european pv output using 30 years of validated hourly reanalysis and satellite data," *Energy*, vol. 114, pp. 1251-1265, Nov. 2016.
[32] J. A. Jardini, C. M. V. Tahan, M. R. Gouvea *et al*., "Daily load profiles for residential, commercial and industrial low voltage consumers," *IEEE Transactions on Power Delivery*, vol. 15, no. 1, pp. 375-380, Jan. 2000.

Dejan P. Jovanović received the B.Sc. (Dipl. Ing.) degree in electrical and microelectronic engineering and the M.Sc. degree in system control engineering from the University of Belgrade, Belgrade, Serbia, in 1996 and 2002, respectively, and the Ph.D. degree in statistics from the University of Queensland, Brisbane, Australia, in 2014. His research interests include control systems, power electronics, and application of machine learning in fault diagnosis and fault-tolerant control.

Gerard F. Ledwich received the Ph. D. degree in electrical engineering from the University of Newcastle, Newcastle, Australia, in 1976. He is currently a Research Professor of electric power with the School of Electrical Engineering and Robotics, Queensland University of Technology, Brisbane, Australia. He has 215 journal publications and 323 refereed conference publications. He has a Scopus H-index of 44 and a citation count of 8633. He has been involved in securing grants of more than AU$16 million with the majority of them were in explicit partnership with industry. His research interests include power systems, power electronics, and wide area control of smart grid.

Geoffrey R. Walker received the B.E. and Ph.D. degrees from The University of Queensland (UQ), Brisbane, Australia, in 1990 and 1999, respectively. From 1998 to 2007, he was the Power Electronics Lecturer with UQ. From 2008 to 2013, he was a Senior Electrical Engineering Consultant with Aurecon's Transmission and Distribution Group, Brisbane, Australia, across various areas, including rail traction, grounding studies, electricity transmission planning, and renewable energy project design and review. In 2013, he joined the Electrical Power Engineering Group, Queensland University of Technology, Brisbane, Australia, as an Associate Professor. His current research interests include applying power electronics to applications in renewable energy (especially photovoltaic), power systems, and electric vehicles.